DETERMINATION OF SPRAY ANGLE AND FLOW UNIFORMITY OF SPRAY NOZZLES WITH IMAGE PROCESSING OPERATIONS

N. Çetin[1*], C. Sağlam[1] and B. Demir[2]

[1]Department of Biosystems Engineering, Faculty of Agriculture, University of Erciyes, 38039 Kayseri, Turkey
[2]Department of Mechanicaland Metal Technologies, Vocational School of Technical Sciences, University of Mersin, 33343 Mersin, Turkey
[*]Corresponding Author Email: necaticetin@erciyes.edu.tr

ABSTRACT

This study was conducted to determine the spray angle and flow uniformity of different hydraulic spray nozzles at different spray pressures with the aid of image processing operations. Spray images were captured with a digital camera to determine spray angles and spray patterns. Captured images were transferred to computer environment and analyzed with different image processing software. The spray angle at 3 bar pressure was measured as 107.2º for anti-drift nozzles, as 105.6º for air-injection nozzles, as 69.9º for ST 80 flat-fan nozzles, as 84.0º for ST 90 flat-fan nozzles, as 103.2º for ST 110 flat-fan nozzles and as 54.2° for hollow-cone Ø1.0 mm nozzles. Cone angle at 3 bar pressure was measured as 106.7º for anti-drift nozzles, as 103.9º for air-injection nozzles, as 75.1º for ST 80 flat-fan nozzles, as 86.4º for ST 90 flat-fan nozzles, as 105.2º for ST 110 flat-fan nozzles and as 46.4º for hollow-cone Ø1.0 mm nozzles. Spray pattern obtained with the image processing method was identical with the flow uniformity obtained with line-profile method. It was concluded that spray pressures had significant effects on spray angles (p $\leq$0.05) of all nozzles.

Keywords: Cone angle, image processing, pressure, spray angle, spray pattern.

INTRODUCTION

Chemicals are used as the most common disease, pest and weed control practice since it is easy to apply, they are fast-acting and quite effective on undesired agents. Unconscious and improper pesticide treatments may have negative impacts on environment, ecosystem and human health. Such unconscious uses also result in pesticide losses and resultant excessive uses bring an extra cost to producers (Demir, 2015).

In chemical treatments, pests and diseases should be properly identified, the practice should be economic and the method of treatment and pesticide to be applied should be properly selected. Besides these requirements, selection of treatment unit spraying chemicals onto the target also plays a significant role in success of treatment. The primary target of spraying process is to have a homogeneous spread over the plant, to retain the pesticide over the plant, to reduce changes in pesticide distribution and drifts and to get the greatest biologic efficiency at recommended dose of application. In this sense, proper use of treatment unit at proper conditions allows the best practice of chemical treatments (Sayıncı, 2008). Various types of nozzles have been designed to improve application performance and efficiency. These nozzles have large spectrum droplet diameters and spray patterns. They usually have varying spray angles (Krishnan et al., 2004).

The sprays used in pesticide treatments (hydraulic sprayers) leave the liquid to the target as droplets at different sizes and speeds (Nuyttens et al., 2007; Sayıncı, 2016). Volumetric distribution uniformity should be measured and checked since it greatly influences droplet trajectory and interaction with the target (Butler Ellis et al., 1997). Spray angle, volumetric uniformity, length of liquid layer and application rate are important spray characteristics effecting pesticide application process (Stafford, 2000; Vulgarakis Minov, 2015).

Droplet spectrum depends on orifice outlet, nozzle spray angle and operating speed and such parameters designate spray quality. Spray coverage, droplet size, application rate and pesticide efficiency influences drift potential of the nozzles (Johnson et al., 2005). Structural characteristics of spray units, operating parameters, meteorological parameters, plant characteristics and physical characteristics of the liquid to be delivered are the important parameters effecting treatment performance (Sayıncı and Bastaban, 2009). Spray angle is commonly used in assessing treatment performance of spray nozzles. Sprays mostly have a conical pattern. Cone angle is defined as the angle between tangential of spray envelope at nozzle outlet (Shafaee, 2011). Spray angles are generally influenced by nozzle dimensions, liquid characteristics and density of the ambient to which the liquid was sprayed (Sayıncı, 2016).

Together with recent developments in computer technology, image procession has started to be used in various processes. In image processing, still or mobile

images captured by a camera or scanner is subjected to digital conversion and these numeric data are interpreted with the aid of different algorithms. In sustainable agriculture, image processing is used to calculate leaf area index, to monitor plant growth and development, to determine maturation times of fruits and vegetables through color analyses, to classify agricultural products and to identify weeds for chemical application (Demir *et al.*, 2016).

This study was carried out to determine the changes in spray pattern, spray and cone angle of spray nozzles at different pressures with image processing operations. Spray angles of hydraulic nozzles were compared with nominal angle values. The similarities between the spray patterns determined with image processing operations and flow uniformity charts determined with line profile method were also assessed.

MATERIALS AND METHODS

Material: This study was conducted at laboratories of Agricultural Machinery and Technologies Department of Agricultural Faculty in Atatürk University. A patternator designed by Çömlek (2017), spray handle and a camera were used to determine spray angle, nozzle flow rate, coverage width and spray pattern. Resultant images were transferred to computer and changes in relevant parameters were determined with the aid of image processing techniques.

Sprayer: Experiments were conducted in the patternator (Çömlek, 2017) and a field sprayer (TP 200 Piton, Taral®, TR) equipped with 200 liters polyethylene tank was used for the spray line. The pressure regulator of the outlet line (maximum 40 bar, 90 L min^{-1}, RG-7 Model) is controlled by a glycerin-filled variable monometer (Pakkens® Model, TR) with a spray pressure indicator of 0 – 25.0 bar. The piston-membrane-type pump delivering the fluid into spray line (TAR30, Taral®, TR) is able to reach 30 L min^{-1} nominal flow rate at 39.2 bar (40 kg cm^{-2}) nominal pressure. Because of long operating durations, the pump was dismantled from the sprayer frame. Pump shaft was connected to belt drive mechanism with an electric motor (2.2 kW, 1405 rpm, AGM 100L 4a type, Gamak, TR). Pump shaft speed was measured with an optic tachometer as 500 rpm.

Nozzle types: In this study, anti-drift nozzles (AD 120-015, AD 120-03, AD 120-04), air-injection nozzles (AI 120-015, AI 120-02 and AI 120-03), standard flat-fan nozzles (ST 80-03, ST 90-04, ST 110-01, ST 110-02, ST 110-03 and ST 110-04) and hollow-cone nozzles (HC Ø1.0 mm, HC Ø1.2 mm and HC Ø1.5 mm) were used.

Imaging equipment: A digital SLR camera (Nikon D300, JP) was used to capture spray images. The camera was mounted on a tripod and images were captured in a fixed position. A black background was placed behind the spray nozzle to have clear images. Two para-flashes equipped with a soft box were positioned toward to spray nozzles to light spray beam. In this way, high-contrast images were obtained at low light intensities. To capture the sprays of nozzles sequenced over a spray boom, 300 cm rail was constructed, and rail vehicle-mounted camera moved over these rails.

Single nozzle patternator: Patternator is a surface composed of leak-proof corrugations placed side-by-side. The liquid flowing through the corrugations at a certain pressure and height conditions is collected in measurement cups (ml). These volumes are placed on ordinate (*y*-axis) and the distances of the corrugations either right or left of the nozzle center line are placed on apsis (*x*-axis). In this way, volumetric distribution shape (spray pattern) is obtained. In this study, a patternator made of chromium plated sheet with 60 canals (canal spacing 20.5 mm), total width of 120 cm and a height of 100 cm and able to spray from a single nozzle was used to determine flow characteristics. Patternator canals have a height of 80 mm and manufactured as portable fashion. Spray height can be adjusted at between 20 - 90 cm. Patternator canals were installed at 10% slope to main frame. The liquid collected within the canals initially transferred to fluid conveyance line and then to 25 ml graduated polystyrene burettes through rubber pipes.

Spraying parts and nozzle flow rate: Spray nozzle was mounted on 3-outlet membrane-type nozzle body (Arag SRL 40642W7 Model, IT). Spray pressure was checked from a glycerin-filled manometer (Pakkens® MG050GRS1 Model, TR) with maximum 10 bar indicator mounted quite close to the nozzle. Flow was controlled by a diaphragm-type solenoid valve (SMS-TORK S1020 type, TR). Nozzle flow rate was measured at different spray pressures with a digital flow meter (Sprayer Calibrator, SpotOn®, Model: SC-1, 1L, range of measurement: 0.08-3.79 L min^{-1}).

Method

Determination of spray angle: High-contrast spray images obtained at nozzle orifice outlet with the aid of artificial light toward to spray beam at dark are presented in Figure 1. Over these images, angle module of ImageJ v.1.38x (Wayne Rasband, National Institutes of Health, US, 2006) image processing software was used to determine spray angle at the nozzle orifice outlet. Nominal angle represents the manufacturer-specified angle valid under certain operating conditions.
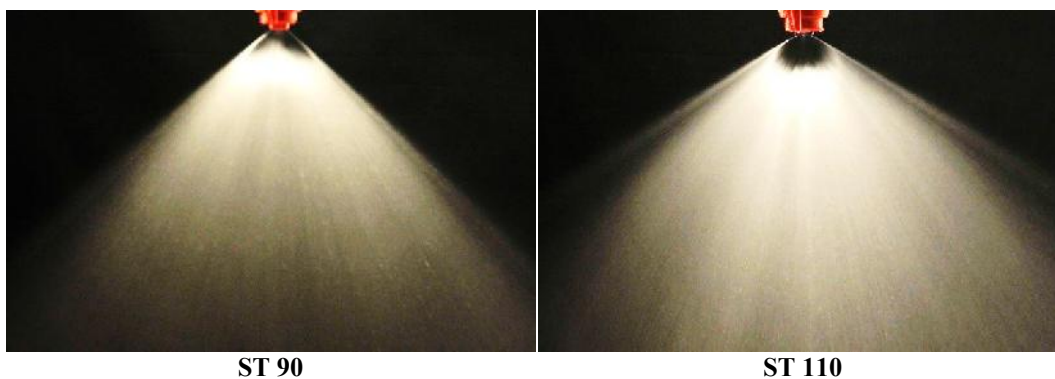
ST 90   ST 110
Figure 1. Spray images obtained at 3 bar spray pressure.

Determination of spray pattern: Spray patterns of 15 spray nozzles at fixed position were determined with the aid of 1200×1000×20.5 mm single nozzle patternator with 60 canals. Spray height was adjusted as 40 cm for anti-drift nozzles and ST 110-type nozzles, as 60 cm for ST 80, ST 90 and hollow-cone nozzles and sprays were performed at 12 different pressures (1 - 12 bar) for hollow-cone nozzles and at 8 different pressures (1 - 8 bar) for the other nozzles. Experiments were conducted in six replications for hollow-cone nozzles, in two replications for ST 90-type nozzles, in three replications for anti-drift and ST 80 and ST 110 type nozzles. Sprays were terminated when 90% of measuring tubes was filled and the marking balls inside the tubes generated the spray pattern. Spray pattern images ([*].jpeg) were taken with the aid of a digital camera (Panasonic Lumix DMC-FZ50, JP) mounted onto a tripod from 2.5 m distance from the spray. Over these images, numbers of full tubes were determined and volumetric cover width for a certain spray height was calculated (number of full tubes × canal distance (2.05 cm)). Over spray pattern images, the height of liquid flowed into the tube from each canal was determined in pixels on *y*-axis with the aid of an image processing software (CMEIAS Image Tool Ver. 1.28,

USA, Liu *et al., 2001*) and ultimately spray patterns were obtained.

Determination of flow uniformity with the line profile method: Spray angle images were transferred to MATLAB R2009 to determine flow uniformity. Flow uniformity graphs were generated for 350th line on the same "*x*" axis (apsis) of each image. Over the images taken through artificial light at dark environment, the color fluctuations (gray toning, between 0-255) over the line reflecting the differences in liquid volumes of spray beam were used to generate the graphs. This method used in determination of flow uniformity was tried for the first time. Replicated measurements were more practical than the other method. Better flow uniformity was achieved at different nozzles and different pressures through changing the position of line bar over the apsis axis (Çetin, 2017). However, in this study, to have an idea, graphs were generated over the same line in all images. The graphs generated at different pressures (2.0, 4.0 and 6.0 bars) were compared with the spray pattern graphs obtained with the aid of CMEIAS Image Tool Ver. 1.28 (Liu *et al., 2001*) at the same pressured.
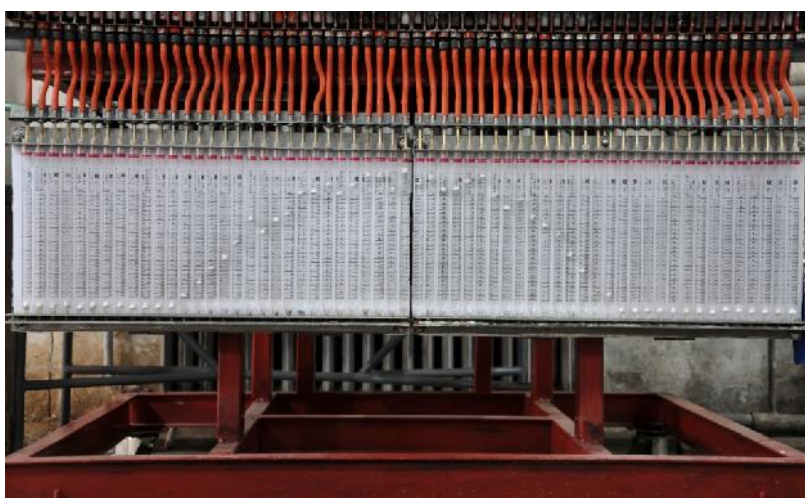

Figure 2. Spray pattern on patternator

Determination of cone angle: Cover width at a certain spray height (40 and 60 cm) was calculated by using Equation 1. Cover width (*b*, cm) was calculated by multiplying the distance between two canals (*m_k*) with the number of tubes used to obtained spray pattern (*n_k*). Nozzle cone angle (*α°*) at constant operating pressure and spray height (*h*, cm) was calculated by using the Equation 2.

$$b = m_k \times n_k \qquad (1)$$

$$\alpha = 2 \times tan^{-1}\left(\frac{b}{2 \times h}\right) \qquad (2)$$

where;

α : Cone angle (°),
b   : Cover width (cm, number of full tubes × distance between two patternator canals),
h   : Spray height (cm),
m_k   : Distance between two patternator canals (cm),
n_k   : Number of tubes used to obtain spray pattern.

Determination of nozzle flow rate: Nozzle flow rates were measured at 6 different spray pressures (2.0, 4.0, 6.0, 8.0, 10.0 and 12.0 bars) for hollow-cone nozzles and at 4 different spray pressures (2.0, 4.0, 6.0 and 8.0 bars) for the other nozzle types. Nozzle flow rates were measured in 3 replicated with the aid of a digital flow meter (Sprayer Calibrator, SpotOn®, Model: SC-1, 1L) with a measurement range of 0.08 - 3.79 L min⁻¹. Mean flow rates and standard deviations were provided in tables and the relationships between the square root of spray pressure and flow rate were presented in graphs and linear equations.

Nozzle and pressure dependent spray angles and nozzle flow rates were also subjected to regression analysis and means were compared at significance level P≤0.05. Statistical analyses were performed with SPSS 20.0 statistical software (IBM SPSS® 2010). Tukey grouping among spray pressures and spray angles for different nozzle types was conducted by using SAS Version 8.02 software (SAS Institute, Cary, NC, USA, 1999).

RESULTS AND DISCUSSION

In this study, the effects of different nozzle types (AD, AI, ST and HC) and different spray pressures on spray and cone angle and spray pattern were investigated through image processing technique.

Nozzle flow rate: Mean flow rates and standard deviations measured for different nozzle types at different spray pressures (2.0, 4.0, 6.0, 8.0, 10.0 and 12.0 bars) are provided in Table 1. Mean flow rates varied between 0.49-2.65 L min⁻¹ for anti-drift nozzles (AD), between 0.48-1.97 L min⁻¹ for air-injection nozzles (AI), between

0.31-2.29 L min⁻¹ for standard flat-fan nozzles (ST) and between 0.53-1.92 L min⁻¹ for hollow-cone nozzles (HC).

Spray angle: The changes in spray angles of anti-drift and air-injection nozzles at 8 different pressures are provided in Table 2. Mean spray angles of anti-drift nozzles varied between 94.6-121.4°. The closest values to the nominal angle were obtained at 7-8 bar spray pressures. Mean spray angles of air-injection nozzles varied between 85.5-124.3°. Dorr *et al.* (2013) reported spray angle of AI 110-015-type nozzle as 124° at 150 kPa and as 150° at 450 kPa.

The changes in spray angle values of standard flat-fan nozzles at 4 different orifice size and 8 different spray pressures are provided in Table 3. Nominal angle is specified as 110° for this type of nozzle. The closest values to the nominal value were obtained at 3-4 bar pressures. Regarding orifice sizes, the closest values were achieved at 03 gpm (gallons per minute) orifice size.

Hollow-cone nozzles had the narrowest spray angles. Any nominal angles were not specified by the manufacturer for this type of nozzle. Spray angles were tested at 3 different nozzle plates (Ø1.0 mm, Ø1.2 mm Ø1.5 mm) and 12 different pressures (Table 4). In HC Ø1.0 mm nozzle, the narrowest angle was measured as 40.1° and the largest angle was measured as 57.8°. Spray angles of HC Ø1.2 mm nozzle varied between 46.4-67.7°. The largest spray angles were measured in HC Ø1.5 mm nozzle and the values varied between 55.0-76.1°. Increasing spray angles were observed with increasing orifice diameter of these nozzles.

Pressure-dependent changes in spray angles of narrow cone standard flat-fan ST 80-03 and ST 90-04 nozzles are provided in Table 5. Spray angles of ST 80-03 nozzle varied between 56.4-80.2°. The closest values to nominal angle of ST 90-04 nozzle (90°) were achieved at 4-5 bar pressures. Standard deviations in nozzle type were quite low. Vulgarakis Minov (2015) reported pressure-dependent spray angles of ATR 80-type orange nozzles as between 92.4-101.6°.

Statistics for spray angles measured at different spray pressures of all nozzle types are provided in Table 7. There were cubic polynomial relationships with high R² values between spray pressure and spray angle and resultant regression equations are provided in Table 7.

Cone angle: Nominal angles, cone angles calculated from the equations at 3 bar and spray angles are provided in Table 8. Both the spray angle and the cone angle of ST 90-04 and ST 110 nozzles were close to nominal angle. In general, cone angles of all nozzles were matching up with spray angles. Çömlek (2017) reported cone angle as 81.2° for HC Ø1.0 mm nozzle, 79.9° for HC Ø1.6 mm nozzle and 93.8° for HC Ø2.4 mm. Vulgarakis Minov (2015) reported cone angles at different heights (0, 15, 30 and 50 cm) and 400 kPa pressure as between 108.5-110.8° for XR 110-01 nozzles, as between 113.8-119.0°

for XR 110-02 nozzles and as between 117.5-120.1° for XR 110-04 nozzles. Mengeş (1995) reported cone angles of flat-fan nozzles at different pressures (200, 300 and 400 kPa) as between 98-123º.

Spray pattern: Spray pattern images were obtained from the flows over a single nozzle patternator. In general, hydraulic spray nozzles have triangle, trapezoidal and rectangular patterns.

Spray patterns generated with the aid of CMEIAS Image Tool Ver. 1.28 and MATLAB software are presented in Figure 3. Two different methods were used to determine spray patterns. In the first method,

coordinates of marking balls were determined and converted into numeric data (pixel) to generate spray pattern. In the second method, instead of spray pattern images, spray angle images obtained at the same pressures were transferred to MATLAB and color fluctuation-dependent flow uniformity graphs were obtained with the aid of line profile method from the same line over the apsis axis of each image. The graphs drawn with the aid of line profile method took less time than the other method. Spray pattern and flow uniformity graphs of all nozzles were coincided with each other.

Table 1. Flow rates of different nozzles at different pressures.

Nozzle type	Pressure (bar)	Flow rate±SD (L min⁻¹)	[1]Nozzle type	Pressure (bar)	Flow rate±SD (L min⁻¹)
AD 120-015	2	0.49±0.01	ST 110-01	2	0.31±0.02
	4	0.69±0.00		4	0.44±0.03
	6	0.87±0.01		6	0.54±0.03
	8	1.00±0.02		8	0.63±0.04
AD 120-03	2	0.96±0.01	ST 110-02	2	0.60±0.02
	4	1.37±0.01		4	0.84±0.03
	6	1.71±0.03		6	1.06±0.04
	8	1.99±0.03		8	1.24±0.04
AD 120-04	2	1.26±0.03	ST 110-03	2	0.91±0.01
	4	1.80±0.03		4	1.26±0.03
	6	2.30±0.04		6	1.60±0.05
	8	2.65±0.09		8	1.84±0.06
AI 120-015	2	0.48±0.01	ST 110-04	2	1.22±0.02
	4	0.69±0.01		4	1.73±0.03
	6	0.85±0.01		6	2.17±0.05
	8	0.99±0.02		8	2.26±0.05
AI 120-02	2	0.64±0.01	ST 80-03	2	1.22±0.08
	4	0.92±0.01		4	1.79±0.19
	6	1.14±0.01		6	2.14±0.12
	8	1.32±0.01		8	2.25±0.11
AI 120-03	2	0.95±0.02	ST 90-04	2	1.23±0.00
	4	1.34±0.02		4	1.74±0.02
	6	1.69±0.03		6	2.18±0.05
	8	1.97±0.03		8	2.29±0.03
HC Ø1.0 mm	2	0.53±0.04	HC Ø1.5 mm	2	0.82±0.04
	4	0.73±0.05		4	1.11±0.07
	6	0.87±0.02		6	1.36±0.06
	8	1.00±0.03		8	1.57±0.08
	10	1.06±0.03		10	1.72±0.10
	12	1.17±0.04		12	1.92±0.10
HC Ø1.2 mm	2	0.68±0.04			
	4	0.95±0.06			
	6	1.14±0.06			
	8	1.29±0.07			
	10	1.40±0.09			
	12	1.55±0.08			

Table 2. Pressure-dependent spray angle (º) values (Mean ± SD) of anti-drift and air-injection nozzles.

Spray pressure (bar)	AD 120-015	AD 120-03	AD 120-04
1	92.3^d±3.5	89.3^e±5.1	102.2^b±5.1
2	105.5^c±4.2	100.2^d±1.6	111.2^{sb}±4.6
3	113.3^{bc}±4.6	105.6^{cd}±0.5	115.3^a±2.4
4	115.0^{abc}±3.0	107.9^{bcd}±2.2	117.7^a±4.5
5	120.5^{ab}±2.1	113.1^{abc}±2.2	119.0^a±2.1
6	121.8^{ab}±3.3	114.4^{abc}±4.6	118.7^a±2.8
7	122.6^{ab}±3.6	115.4^{ab}±4.1	120.0^a±3.1
8	123.7^a±1.9	119.1^a±2.1	121.4^a±5.1
Spray pressure (bar)	AI 120-015	AI 120-02	AI 120-03
1	75.9^e±4.8	85.3^b±3.0	95.4^e±4.1
2	100.9^d±2.8	97.9^{ab}±4.1	106.5^d±2.8
3	112.8^c±2.6	106.6^a±2.4	112.9^{cd}±1.8
4	120.3^{bc}±0.7	113.4^a±5.0	115.4^{bc}±1.4
5	125.4^{ab}±3.4	116.4^a±1.8	119.3^{abc}±3.4
6	126.6^{ab}±2.0	116.4^a±9.0	120.7^{ab}±0.6
7	129.2^a±2.6	116.7^a±10.5	123.6^a±0.2
8	132.9^a±2.4	116.7^a±10.4	123.4^a±3.1

*Different letters on same column show significant difference (P ≤ 0.05)

Table 3. Pressure-dependent spray angle (º) values (Mean ± SD) of standard flat-fan nozzles.

Spray pressure (bar)	ST 110-01	ST 110-02	ST 110-03	ST 110-04
1	87.5^d±7.6	70.5^d±5.6	91.5^d±3.1	102.0^d±5.2
2	103.1^c±0.4	89.5^c±4.7	102.8^c±4.4	109.0^{cd}±3.3
3	108.9^{bc}±3.2	100.2^{bc}±4.9	107.0^{bc}±3.5	113.3^{bc}±1.7
4	117.1^{ab}±3.6	103.8^{ab}±3.9	111.2^{ab}±2.5	116.9^{ab}±1.3
5	118.5^{ab}±2.9	107.0^{ab}±5.3	112.7^{ab}±2.2	118.5^{ab}±0.9
6	119.4^{ab}±2.7	109.9^{ab}±2.8	115.9^a±2.1	119.2^{ab}±1.0
7	120.4^a±2.8	111.0^{ab}±3.7	116.9^a±2.6	119.7^{ab}±1.7
8	121.6^a±2.6	114.5^a±2.5	117.5^a±2.5	120.9^a±1.1

*Different letters on same column show significant difference (P ≤ 0.05)

Table 1. Pressure-dependent spray angle (º) values (Mean ± SD) of hollow-cone nozzles.

Spray pressure (bar)*	HC Ø1.0 mm	HC Ø1.2 mm	HC Ø1.5 mm
1	40.1^b±8.7	46.4^d±3.9	55.0^c±5.0
2	44.9^{ab}±8.0	54.0^{cd}±4.1	63.4^{bc}±5.8
3	48.5^{ab}±7.0	58.8^{bc}±3.3	68.7^{ab}±5.5
4	51.9^{ab}±8.5	62.4^{ab}±3.9	70.6^{ab}±5.3
5	51.9^{ab}±8.7	63.2^{ab}±3.5	72.6^{ab}±5.6
6	53.7^{ab}±9.4	64.2^{ab}±3.4	73.7^{ab}±4.5
7	54.0^{ab}±8.3	65.4^{ab}±4.1	73.8^a±4.5
8	55.1^{ab}±7.0	66.3^{ab}±4.0	74.4^a±4.7
9	55.7^{ab}±8.4	67.1^a±4.7	74.9^a±5.0
10	56.2^{ab}±8.4	67.2^a±4.9	75.5^a±4.6
11	57.3^a±9.2	67.7^a±4.3	75.4^a±3.7
12	57.8^a±9.1	67.7^a±4.1	76.1^a±4.3

*Different letters on same column show significant difference (P ≤ 0.05)

Table 2. Pressure-dependent spray angle (º) values (Mean ± SD) of narrow-cone standard flat fan nozzles.

Spray pressure (bar)	ST 80-03	ST 90-04
1	56.4^b±4.6	74.4^e±0.7
2	68.3^{ab}±2.7	81.9^d±1.3
3	71.9^a±4.5	85.5^c±0.4
4	76.2^a±4.7	89.5^b±1.4
5	79.1^a±5.3	90.4^{ab}±0.5
6	79.9^a±5.1	91.8^{ab}±0.2
7	79.6^a±3.6	92.6^a±0.4
8	80.2^a±3.9	93.1^a±0.3

[*]Different letters on same column show significant difference (P ≤ 0.05)
In all nozzle types, the effects of spray pressure on spray angle were found to be highly significant (p≤0.01) (Table 6).

Table 3. Regression analysis results.

[1]Nozzle type	Statistics	SD	MS	F	p (sigma)
AD	Regression	3	183.665	241.38	0.000[**]
	Error	4	0.761		
	Total	7			
AI	Regression	3	416.247	1089.46	0.000
	Error	4	0.382		
	Total	7			
HC Ø1.0mm	Regression	3	103.689	344.58	0.000
	Error	8	0.301		
	Total	11			
HC Ø1.2mm	Regression	3	154.330	245.37	0.000
	Error	8	0.629		
	Total	11			
HC Ø1.5mm	Regression	3	141.218	230.83	0.000
	Error	8	0.612		
	Total	11			
ST 90-04	Regression	3	98.198	404.75	0.000
	Error	4	0.243		
	Total	7			
ST 110	Regression	3	251.497	624.64	0.000
	Error	4	0.403		
	Total	7			
ST 80-03	Regression	3	159.138	126.67	0.000
	Error	4	1.256		
	Total	7			

[**] Highly significant (p≤0.01)
[1]AD: Anti-Drift nozzle, AI: Air-Injection nozzle, HC: Hollow-Cone nozzle, ST: Standard Flat-Fan nozzle

Table 4. Relationships between spray pressure and spray angle.
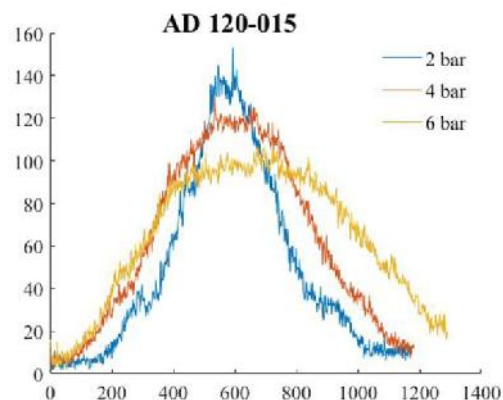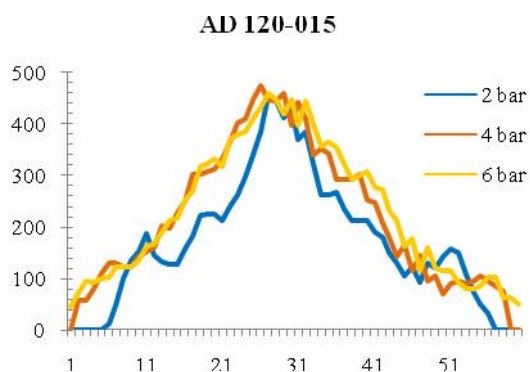
Nozzle type	[*]Equation	R^2
AD	$y = 0.148x^3 - 2.634x^2 + 16.708x + 80.766$	0.990
AI	$y = 0.200x^3 - 3.809x^2 + 25.191x + 64.271$	0.998
HC Ø1.0 mm	$y = 0.029x^3 - 0.739x^2 + 6.611x + 34.385$	0.989
HC Ø1.2 mm	$y = 0.039x^3 - 1.024x^2 + 9.100x + 39.031$	0.985
HC Ø1.5 mm	$y = 0.048x^3 - 1.209x^2 + 10.029x + 47.019$	0.984

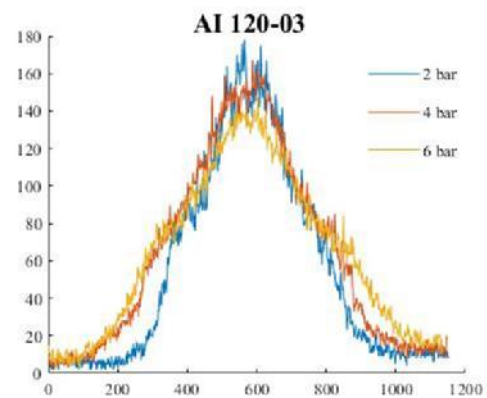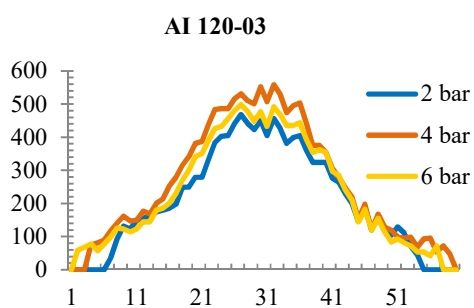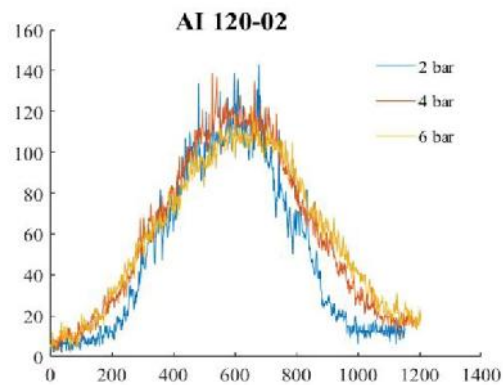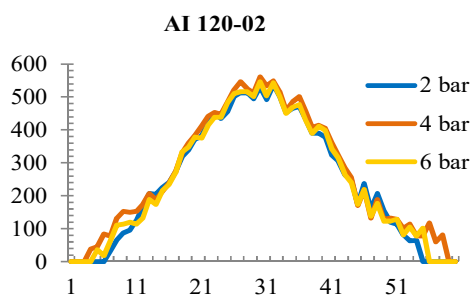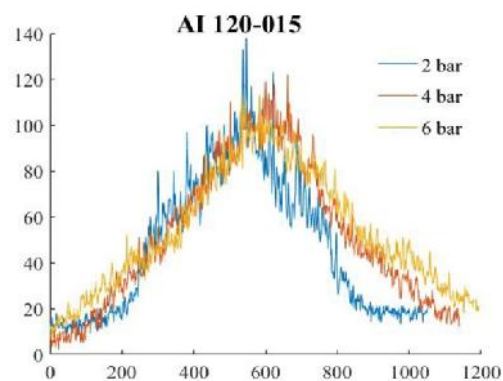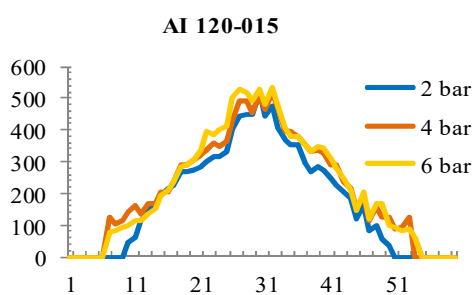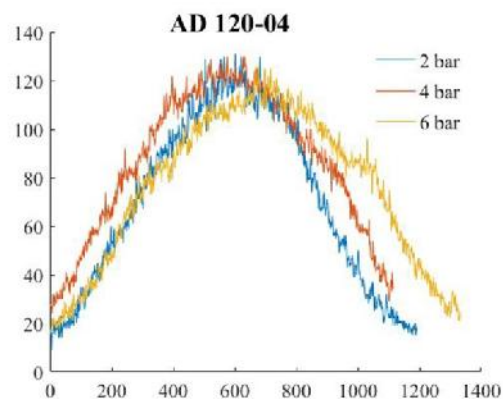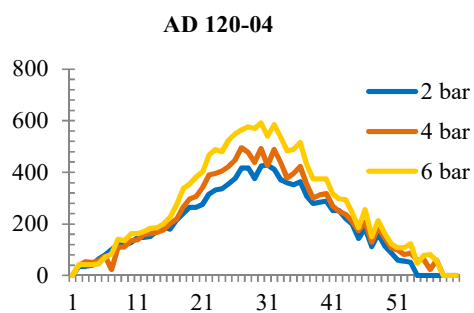|		
ST 80-03	$y = 0.114x^3 - 2.306x^2 + 15.734x + 43.449$	0.982
ST 90-04	$y = 0.078x^3 - 1.554x^2 + 10.963x + 65.056$	0.994
ST 110	$y = 0.173x^3 - 3.166x^2 + 20.216x + 71.001$	0.996

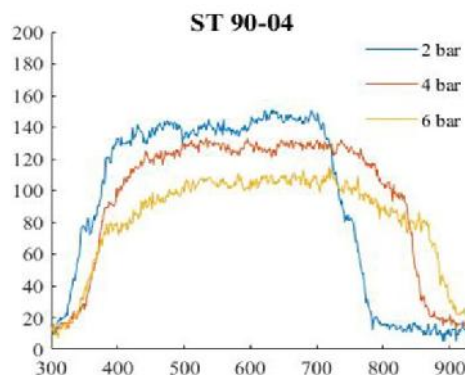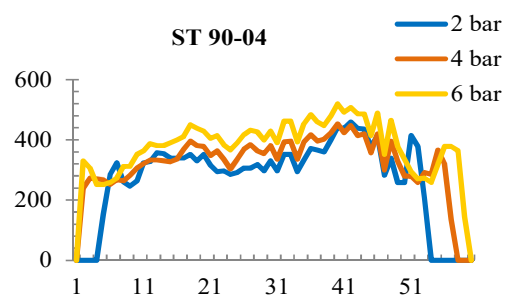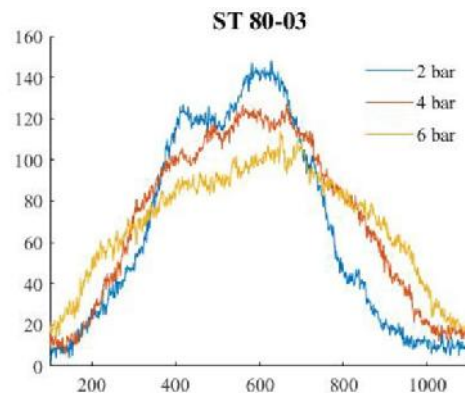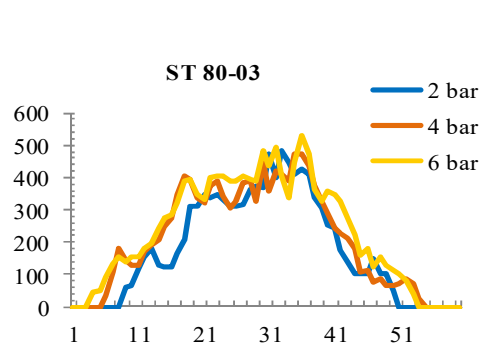[*]: y: Spray angle, x: Spray pressure

Table 5. Nominal angle, spray angle calculated from the equations at 3 bar and cone angles measured at 3 bar.

Nozzle type	Nominal angle (º)	Angle calculated from the equations (º)	Cone angle at 3 bar (º)
AD	120	107.2	106.7±4.9
AI	120	105.6	103.9±4.2
HCØ1.0 mm	-	54.2	46.4±6.6
HCØ1.2 mm	-	57.1	56.7±5.8
HCØ1.5 mm	-	66.2	62.4±5.0
ST 80-03	80	69.9	75.1±2.5
ST 90-04	90	84.0	86.4±2.9
ST 110	110	103.2	105.2±3.7

AD 120-04

AD 120-04

AI 120-015

AI 120-015

AI 120-02

AI 120-02

AI 120-03

AI 120-03

ST 80-03

ST 80-03

ST 90-04

ST 90-04

ST 110-01

ST 110-01

ST 110-02

ST 110-02

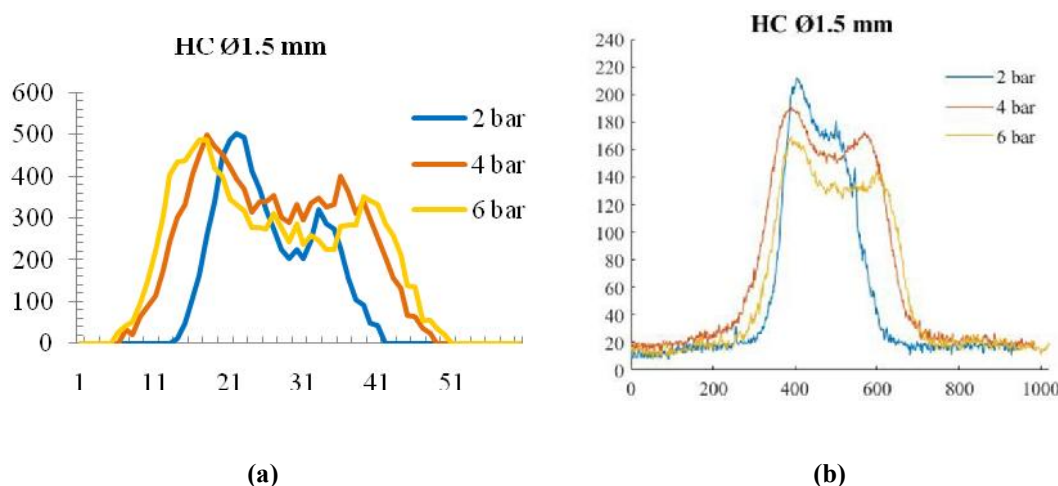(a)   (b)
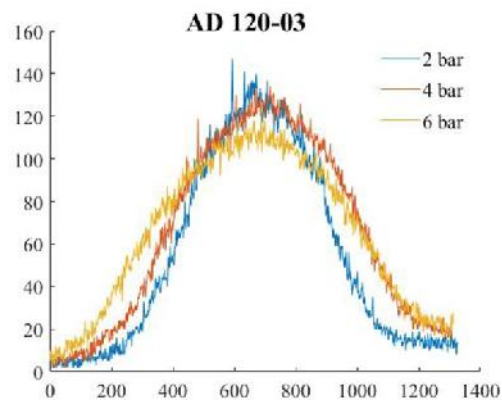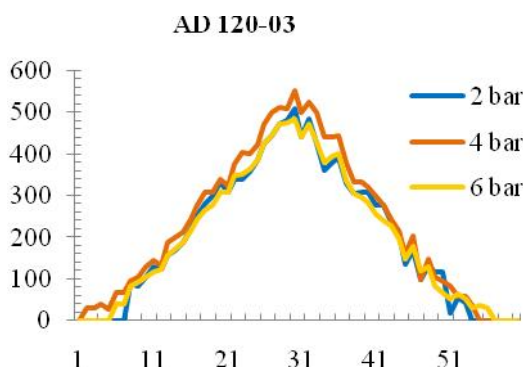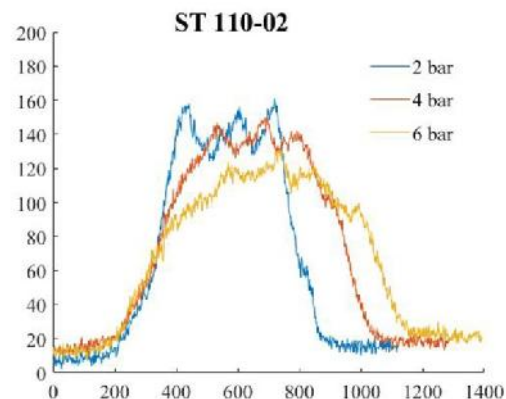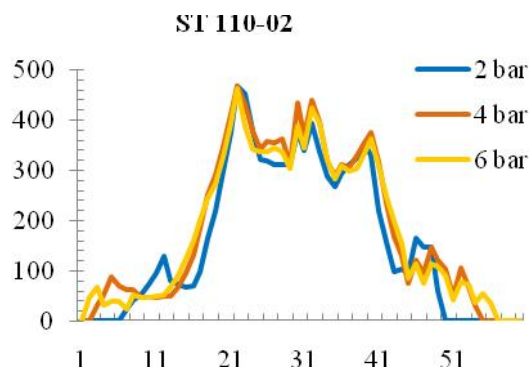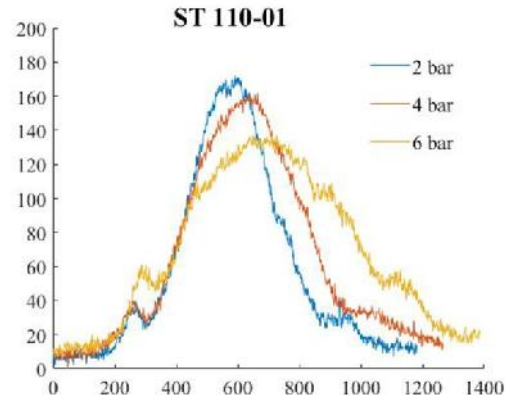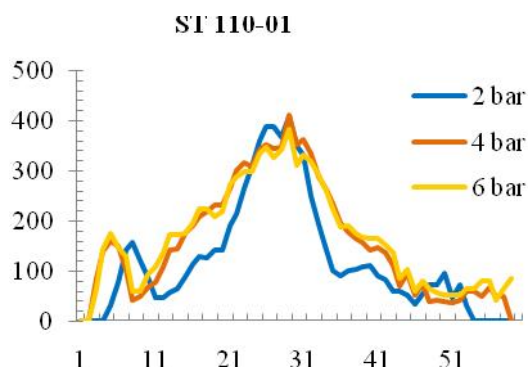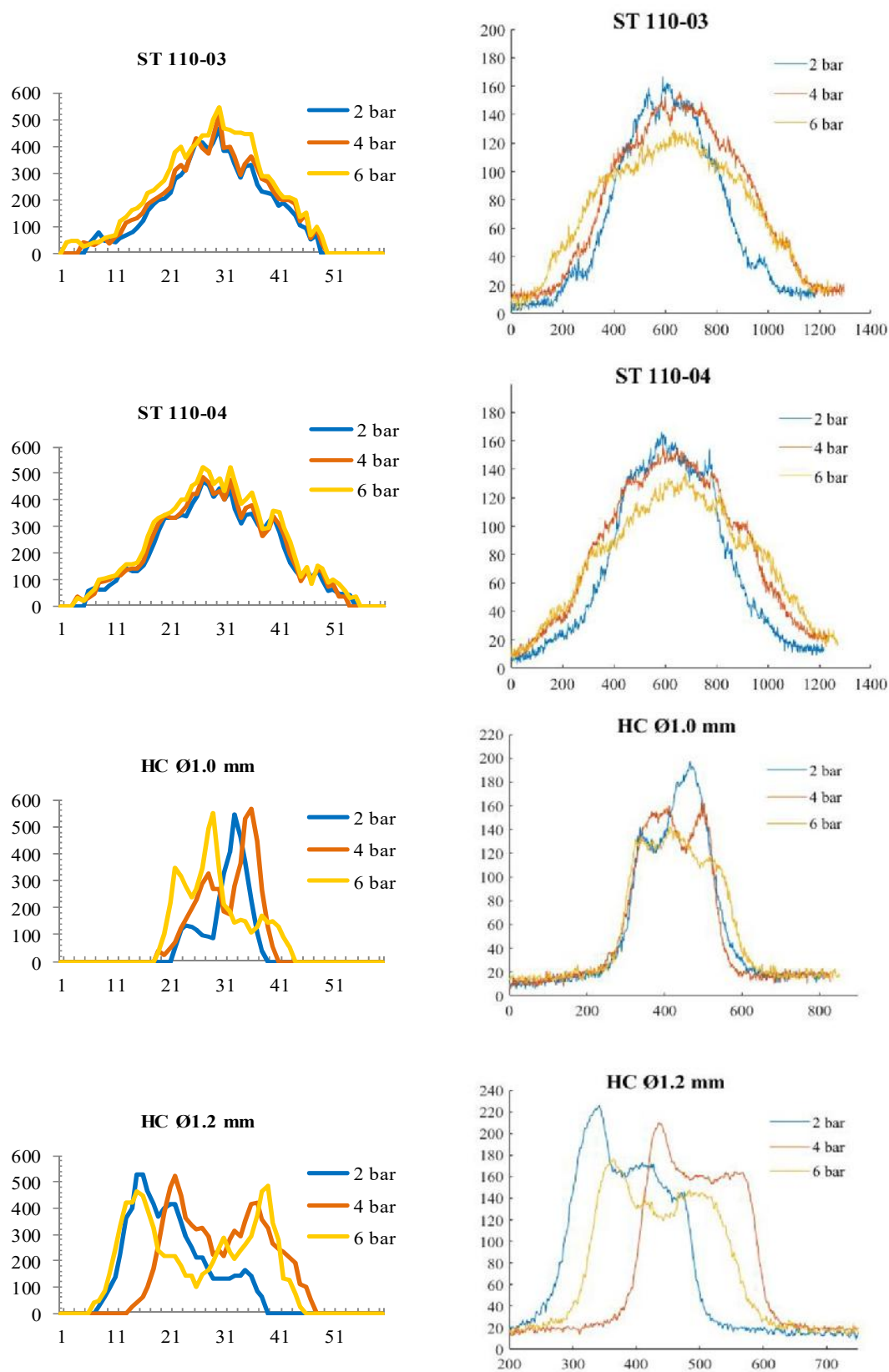
Figure 3. Spray patterns (a) CMEIAS Image Tool Ver. 1.28, (b) MATLAB R2009

Conclusions: Spray and cone angles of different spray hydraulic nozzles were determined under different pressures and resultant values were compared with nominal angles. Present findings revealed that spray angles were closely related to spray pressures. The angle specified over the nozzle body is a nominal value and present angle checks revealed that this value varied with the spray pressure. Spray and cone angle values were close to the nominal angle values under 3 bar spray pressure. There aren't any nominal angle values for hollow-cone nozzles and spray angles increased with increasing orifice diameters. There were not any significant relationships between orifice size and spray angles of standard flat-fan nozzles. Nozzle types were selected among normal and narrow-cone nozzles and the spray angle averages determined with image processing were similar with the cone angle averages determined with patternator.

The increase in spray pressures did not increase spray angles after a certain point, angle values stayed constant and small fluctuations were observed in this value. Zhang *et al.* (2017) indicated a critical injection pressure and spray angles became independent from the spray pressure after this critical value and also indicated that cover width, thus the cone angle will not increase further regardless of the increase in pressure beyond this critical value.

It was proved in this study that spray pattern tests performed in a patternator could also be achieved with image processing operations. MATLAB software was used for image processing and spray pattern was generated with line profile method based on color distribution at a constant height from the nozzle orifice. Resultant spray patterns were compared with the patterns achieved in a patternator operated under the same parameters and quite similar outcomes were achieved. In this sense, a simple and a new method were developed as an alternative to patternator tests. The image processing

operations can be improved to have a simple and practical method to generate spray patterns. There is no need for a special arrangement or equipment, thus the method is also quite economical. The method employed to determine flow uniformity is a first case. The most proper line should be determined in spray images captured from different nozzles at different pressures, then resultant graph will provide better flow uniformity.

All these methods and systems should further be developed to improve the precision of the studies. New applications and technologies should also be developed to get more precise outcomes. Image processing software can be made more specific for this field of study. In this sense, developed systems can determine spray patterns, spray and cone angles from instant video images and complete the process in shorter period and eliminate intuitive preferences of the operator. Operators cannot exhibit the same precision in every image, thus automation should be activated in image processing operations. In this way, measurements will yield more accurate and precise outcomes and quality of the studies will improve.

REFERENCES

Butler Ellis, M. C., C. R. Tuck, and P. C. H. Miller (1997). The effect of some adjuvants on sprays produced by agricultural flat fan nozzles. Crop Protect. 16(1): 41–50.

Çetin, N. (2017). Determination of spraying angle and flow evenness in pulverizator noozles by image processing operation. M. Sc. Thesis. Graduate

School of Natural and Applied Sciences, Erciyes University, Kayseri.

Çömlek, R. (2017). Design, manufacture of spray pattern test unit and flow control of sprayer nozzles. M. Sc. Thesis. Graduate School of Natural and Applied Sciences, Atatürk University, Erzurum.

Demir, B. (2015). A projection for plant protection machinery of central anatolia region. Alınteri J. Agr. Sci. 28(1): 27-32.

Demir, B., N. Çetin, and Z. A. Kuş (2016). Determination of color properties of weed using image processing. Alınteri J. Agric. Sci. 31(B): 59-64.

Dorr, G. J., A. J. Hewitt, S. W. Adkins, J. Hanan, H. Zhang, and B. Noller (2013). A comparison of initial spray characteristics produced by agricultural nozzles. Crop Protect. 53(11): 109-117.

IBM SPSS® (2010). Statistical software. SSS Inc., IBM Company©, Version 20.

ImageJ 1.38x (2006). Image proccessing and analysis in java. USA.

Johnson, P. D., D. A. Rimmer, A. N. I. Garrod, J. E. Helps, and C. Mawdsley (2005). Operator exposure when applying amenity herbicides by all-terrain vehicles and controlled droplet applicators. Annals of Occup. Hyg. 49(1): 25-32.

Krishnan, P., T. Evans, K. Ballal, and L. J. Kemble. (2004). Scanning electron microscopic studies of new and used fan nozzles for agricultural sprayers. App. Engin. in Agric. 20(2): 133-137.

Liu, J., F. B. Dazzo, O. Glagoleva, B. Yu, and A.K. Jain. (2001). CMEIAS: A computer-aided system for the image analysis of bacterial morphotypes in microbial communities. Micr. Eco. 41(3): 173-194 and 42: 215. http://cme.msu.edu/cmeias/

MATLAB (2009) MATLAB & Simulink Release 2009. The MathWorks Inc.

Mengeş, H. O. (1995). The determination of distribution and pulverization characteristics for some different nozzle types used in mechanic field sprayers. M. Sc. Thesis. Graduate School of Natural and Applied Sciences, Selçuk University, Konya.

Nuyttens, D. (2007). Drift from field crop sprayers: The influence of spray application technology determined using indirect and direct drift assessment means. PhD thesis KU Leuven.

SAS (1999). SAS Institute Inc.: SAS Version 8.02: SAS/STAT Software: changes and enhancements through Release 8.02. Cary, NC, SAS Institute Inc, USA.

Sayıncı, B. (2008). Determination of spray application performance into potato canopies with spinning disc and hydraulic spray nozzles, and biological activities with spinosad for *Leptinotarsa decemlineata* say (coleptera: chrysomelidae). PhD Thesis. Graduate School of Natural and Applied Sciences, Atatürk University, Erzurum.

Sayıncı, B. and S. Bastaban (2009). Factors affecting spray application performance of hydraulic nozzles. Turkish J. Sci. Rev. 2(2): 35-41.

Sayıncı, B. (2016). The influence of strainer types on the flow and droplet velocity characteristicsof ceramic flat-fan nozzles. Turkish J. Agric. and Fores. 40(1): 25-37.

Shafaee, M., S. A. Banitabaei, M. Ashjaee, and V. Esfahanian (2011). Effect of flow conditions on spray cone angle of a two-fluid atomizer. J. Mech. Sci. and Tech. 25(2): 365-369.

Stafford, J. V. (2000). Implementing precision agriculture in the 21st century. J. Agric. Engin. Res. 76(3): 267-275.

Vulgarakis Minov S. (2015). Integration of imaging techniques for the quantitative characterization of pesticide sprays. PhD Thesis. Ghent University, Belgium and Burgundy University, France.

Zhang, T., B. Dong, X. Chen, Z. Qiu, R. Jiang, and W. Li, (2017). Spray characteristics of pressure-swirl nozzles at different nozzle diameters. App. Therm. Engin. 121(7): 984-991.